Involvement of the *Phospholipid Sterol Acyltransferase1* in Plant Sterol Homeostasis and Leaf Senescence[1][W]

Pierrette Bouvier-Navé, Anne Berna, Alexandre Noiriel[2], Vincent Compagnon, Anders S. Carlsson, Antoni Banas[3], Sten Stymne, and Hubert Schaller*

Institut de Biologie Moléculaire des Plantes du CNRS, Université de Strasbourg, Département Réseaux Métaboliques Végétaux, F–67083 Strasbourg cedex, France (P.B.-N., A. Berna, A.N., V.C., H.S.); and Department of Plant Breeding and Biotechnology, Swedish University of Agricultural Sciences, S–230 53 Alnarp, Sweden (A.S.C., A. Banas, S.S.)

Genes encoding sterol ester-forming enzymes were recently identified in the Arabidopsis (*Arabidopsis thaliana*) genome. One belongs to a family of six members presenting homologies with the mammalian *Lecithin Cholesterol Acyltransferases*. The other one belongs to the superfamily of *Membrane-Bound O-Acyltransferases*. The physiological functions of these genes, *Phospholipid Sterol Acyltransferase1* (*PSAT1*) and *Acyl-CoA Sterol Acyltransferase1* (*ASAT1*), respectively, were investigated using Arabidopsis mutants. Sterol ester content decreased in leaves of all mutants and was strongly reduced in seeds from plants carrying a *PSAT1*-deficient mutation. The amount of sterol esters in flowers was very close to that of the wild type for all lines studied. This indicated further functional redundancy of sterol acylation in Arabidopsis. We performed feeding experiments in which we supplied sterol precursors to *psat1-1*, *psat1-2*, and *asat1-1* mutants. This triggered the accumulation of sterol esters (stored in cytosolic lipid droplets) in the wild type and the *asat1-1* lines but not in the *psat1-1* and *psat1-2* lines, indicating a major contribution of the PSAT1 in maintaining free sterol homeostasis in plant cell membranes. A clear biological effect associated with the lack of sterol ester formation in the *psat1-1* and *psat1-2* mutants was an early leaf senescence phenotype. Double mutants lacking *PSAT1* and *ASAT1* had identical phenotypes to *psat1* mutants. The results presented here suggest that *PSAT1* plays a role in lipid catabolism as part of the intracellular processes at play in the maintenance of leaf viability during developmental aging.

Sterols are components of most eukaryotic membranes; as such, they are important regulators of membrane fluidity and thus influence membrane properties, functions, and structure (Demel and De Kruyff, 1976; Bloch, 1983; Schuler et al., 1991; Roche et al., 2008). Unlike animals, in which cholesterol is most often the unique end product of sterol biosynthesis, each plant species has its own distribution of sterols, with the three most common phytosterols being sitosterol, stigmasterol, and campesterol (Benveniste, 2004). In addition to their free sterol form, phytosterols are also found as conjugates, particularly fatty acyl sterol esters (SE). Since SE are hardly integrated into the bilayer of the membranes (Hamilton and Small, 1982), the biochemical process of sterol acylation is believed to play a crucial role in maintaining free sterol concentration in the cell membranes (Lewis et al., 1987; Dyas and Goad, 1993; Chang et al., 1997; Sturley, 1997; Schaller, 2004). In other words, SE are generally thought to constitute a storage pool of sterols when those are present in amounts greater than immediately required for the cells. For instance, in plants, accumulation of SE has been described during seed maturation and senescence or when plant cell cultures reach stationary phase (Dyas and Goad, 1993, and refs. therein) as well as in mutant lines overproducing sterols (Gondet et al., 1994; Schaller et al., 1995).

In mammals and yeast, the genes involved in sterol esterification have been known for a long time. These genes encode two types of enzymes responsible for the formation of SE in animals, the Acyl-Coenzyme A: Cholesterol Acyltransferase (ACAT) and the Lecithin: Cholesterol Acyltransferase (LCAT). ACAT, which catalyzes an acyl-CoA-dependent acylation, is a membrane-bound enzyme acting inside the cells (Chang et al., 1997). LCAT, which is evolutionarily unrelated to ACAT, catalyzes transacylation of acyl groups from phospholipids to sterols. It is a soluble enzyme present in the blood stream, where it is an important regulator of circulating cholesterol (Jonas, 2000). The budding

[1] This work was supported by the Centre National de la Recherche Scientifique and by the Agence Nationale de la Recherche (grant no. TERPENE ANR–05–BLAN–0217 to V.C.).

[2] Present address: Institut de Chimie et Biochimie Moléculaires et Supramoléculaires, Université Lyon 1, Bâtiment Chevreul-Porte C227, F–69622 Villeurbanne cedex, France.

[3] Present address: Intercollegiate Faculty of Biotechnology, University of Gdańsk-Medical University of Gdańsk, Kladki 24, 80–822 Gdansk, Poland.

* Corresponding author; e-mail hubert.schaller@ibmp-ulp.u-strasbg.fr.

The author responsible for distribution of materials integral to the findings presented in this article in accordance with the policy described in the Instructions for Authors (www.plantphysiol.org) is: Hubert Schaller (hubert.schaller@ibmp-ulp.u-strasbg.fr).

[W] The online version of this article contains Web-only data.
www.plantphysiol.org/cgi/doi/10.1104/pp.109.145672

yeast *Saccharomyces cerevisiae* has two enzymes of the ACAT type for the synthesis of SE (Yang et al., 1996).

In plants, genes encoding enzymes responsible for SE formation have long been unknown. Based on biochemical studies, it was suggested that phospholipids and/or neutral lipids could serve as acyl donors (Garcia and Mudd, 1978a, 1978b; Zimowski and Wojciechowski, 1981a, 1981b). The identification in the Arabidopsis (*Arabidopsis thaliana*) genome of two genes involved in sterol esterification was based on homology searches. First, the phospholipid:sterol acyltransferase gene *AtPSAT1* (At1g04010) was found to display consistent identity with the mammalian *LCAT* and then was biochemically characterized by expression in Arabidopsis (Noiriel, 2004; Banas et al., 2005). The encoded protein was shown to be associated with microsomal membranes and to catalyze the transfer of unsaturated fatty acyl groups from position *sn-2* of phosphatidylethanolamine (and phosphatidylcholine to a lesser extent) to sterols. The preferred acceptor molecules of PSAT1 were cholesterol, a minor biosynthetic end product in Arabidopsis, then campesterol and sitosterol, the two main end products. Sterol coincubation studies performed with this microsomal enzymatic assay showed that sterol precursors such as cycloartenol or obtusifoliol, which were poor substrates when incubated alone, were preferentially acylated in the presence of sitosterol, suggesting an activation of the enzyme by sitosterol (Banas et al., 2005). Another sterol acyltransferase gene, *AtASAT1* (At3g51970), was identified in a survey of members of the Arabidopsis superfamily of membrane-bound *O*-acyltransferases with a yeast ACAT mutant functional complementation approach (Chen et al., 2007). *AtASAT1* encodes a protein structurally related to the animal and yeast ACATs. This enzyme was shown to prefer saturated fatty acyl-CoAs as acyl donors and cycloartenol as the acyl acceptor. Overexpression of *AtASAT1* in seeds of Arabidopsis resulted in a strong accumulation of cycloartenol fatty acyl esters accompanied by an increase of the whole SE content of these seeds and, in spite of a slight decrease of the free sterol pool, an increase of the total sterol content of the transgenic seeds by up to 60% compared with that of the wild type (Chen et al., 2007). We took advantage of the availability of Arabidopsis T-DNA insertion mutants of these two genes to investigate their respective physiological roles. Here, we report on the involvement of *AtPSAT1* in leaf senescence, its major contribution to SE formation in leaves and seeds, and also its essential role in free sterol homeostasis in these organs.

RESULTS

Isolation of Arabidopsis Mutant Lines Affected in the Expression of Sterol Acyltransferases

Arabidopsis T-DNA insertion lines for At1g04010 (*PSAT1*) and At3g51970 (*ASAT1*) were identified in the SALK and GABI databases, respectively. Schematic representation of T-DNA insertions are shown (Fig. 1A). Genomic PCR analysis of the *psat1-1*, *psat1-2*, and *asat1-1* mutants shown in Supplemental Figure S1 confirmed the insertion sites indicated by the databases. Double mutants *asat1-1/asat1-1*, *psat-1/psat-1*, *asat1-1/asat1-1*, and *psat1-2/psat1-2* were generated by genetic crossing. Homozygous individuals at both *asat1-1* and *psat1-1* or *psat1-2* loci were found in F2 progeny at a 25% frequency, indicating no bias with respect to Mendelian segregation of unlinked genes. Double mutant lines were named *asatpsat1-1* and *asatpsat1-2* for nomenclature convenience. Reverse transcription (RT)-PCR analysis of the wild type and the *asat1-1*, *psat1-1*, and *psat1-2* mutants with total RNA from young growing leaves showed that *asat1-1* is a complete loss-of-function mutant (Fig. 1B, top), whereas *psat1-1* and *psat1-2* mutants were likely to be partial loss-of-function mutants (Fig. 1B, bottom). In fact, it was possible to amplify a PCR product from reverse transcribed RNAs of *psat1-1* with the same size as the PCR product obtained from wild-type reverse transcribed RNAs but in far less abundance (Fig. 1B, bottom). In the case of the *psat1-2* mutant, it was possible to amplify a PCR product that was smaller in size and also far less abundant than the wild-type product (Fig. 1B, bottom). Identical results were obtained with the double mutants. All RT-PCR products were amplified with primers designed to amplify the *PSAT1* open reading frame. Subcloning and sequencing of these RT-PCR products of low abundance obtained from the *psat1-1* and *psat1-2* mutant RNAs showed that several types of cDNAs were present and carried short deletions or nonsense mutations (data not shown). From another RT-PCR analysis of the wild type and *psat1-1* and *psat1-2* mutants (Fig. 1C) also using total leaf RNA as a template but a different *Taq* polymerase (see "Materials and Methods"), we showed that no *PSAT1* mRNA was detected in the case of *psat1-1* and *psat1-2* mutants and that *PSAT1* was expressed at a lower level than *ACTIN2* in the wild type. This latter result was confirmed by real-time quantitative PCR measurements done with RNAs of wild-type leaves (Supplemental Table S2).

Because *PSAT1* and *ASAT1* are ubiquitously expressed (see expression data sets on http://www.genevestigator.ethz.ch), we performed SE measurements for dry seeds, rosette leaves, and flowers. In seeds, SE were found in similar amounts for the wild-type and *asat1-1* genotypes (Fig. 2A). In contrast, levels of SE in *psat1-1*, *asatpsat1-1*, *psat1-2*, and *asatpsat1-2* (data not shown) mutants were 5- to 10-fold reduced when compared with the wild type, showing that PSAT1 had a major effect in SE formation in seeds. Likewise, a slight increase of seed SE was detected in *PSAT1* overexpressor lines (Fig. 2A). The reduced amount of SE in *psat1-1* and *psat1-2* mutant seeds led us to quantify triacylglycerols, the other main neutral lipids found in Arabidopsis seeds. No differences in the total amount of triacylglycerols were found be-

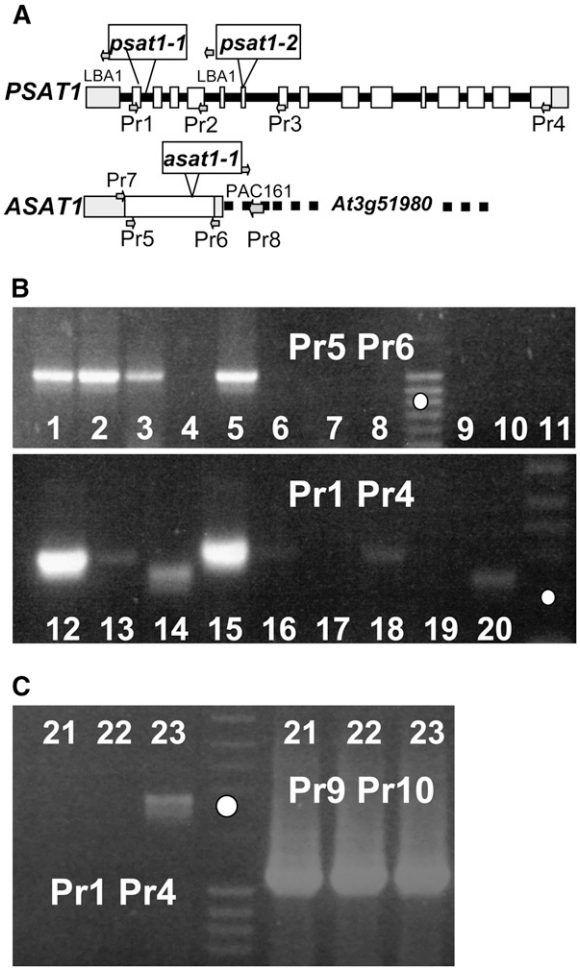

Figure 1. Isolation of loss-of-function mutants for *PSAT1* and *ASAT1*. A, Schematic representation (based on The Arabidopsis Information Resource locus data) of T-DNA insertions in *PSAT1* and *ASAT1* genes. Gray boxes and white boxes indicate nontranslated sequences and exons, respectively. Black lines and dashed black lines indicate introns and other genomic sequences, respectively. T-DNAs appear as inserted frames. Seed stock accessions are as follows: *psat1-1*, SALK_037289; *psat1-2*, SALK_117091; *asat1-1*, GABI_123458. Light gray arrows indicate PCR primers. Primer sequences are given in Supplemental Table S1. B, RT-PCR analysis to confirm loss of function of genes considered here (with Platinum *Taq* DNA polymerase). Top, PCR with primer pair Pr5Pr6 for the detection of *ASAT*. Lane 1, the wild type; lane 2, *psat1-1*; lane 3, *psat1-2*; lane 4, *asat1-1*; lane 5, another wild-type individual plant; lanes 6 to 8, three different *asatpsat1-1* double mutant individual plants; lanes 9 to 11, PCR on the same RT products as in lanes 6 to 8 using *PSAT* promoter-specific primers showing no amplification, as a control of genomic DNA-free samples. The 1.5-kb central band of the DNA ladder is marked with a white dot. Bottom, PCR with primer pair Pr1Pr4 for the detection of *PSAT1*. Lane 12, the wild type; lanes 13 and 16, two distinct *psat1-1* individual plants; lanes 14 and 20, two distinct *psat1-2* individual plants; lane 15, *asat1-1*; lanes 17 and 19, empty lanes; lane 18, *asatpsat1-1* double mutant (showing the same band as in lanes 13 and 16). C, Another RT-PCR analysis (with standard *Taq* DNA polymerase) showing the amplification of *PSAT1* and *ACTIN2* mRNA using primer pairs Pr1Pr4 and Pr9Pr10, respectively. Lane 21, *psat1-1*; lane 22, *psat1-2*; lane 23, the wild type. Equal quantities of RNAs were used in the overall experiments presented here. The high abundance of *ACTIN2* RT-PCR products compared with the low abundance of *PSAT1* RT-PCR products found in young leaf material was confirmed in quantitative real-time RT-PCR experiments (see "Materials and Methods"; Fig. 4D; Supplemental Table S2).

tween the wild type and any of the mutant lines considered in this study (Supplemental Fig. S2). SE levels decreased in leaves of all mutant genotypes analyzed, indicating a role for both ASAT1 and PSAT1 in sterol acylation (Fig. 2B). Finally, levels of SE found in flowers were similar for all genotypes, including the wild type (Fig. 2C), pointing out the contribution of other putative sterol acyltransferases in the formation of SE during the course of plant development. The sterol composition of the SE fractions from rosette leaves of the wild type and *psat1-1* and *psat1-2* mutants is shown as an example in Figure 2D. Pathway end products (24-alkyl-Δ^5-sterols) dominated compared with biosynthetic intermediates, and this was also the case for the other tissues (data not shown).

psat1 Mutants Exhibit an Early Leaf Senescence Phenotype

Arabidopsis lines described in this paper were carefully examined for morphological or cellular phenotypes associated with a loss of function of *PSAT1* or *ASAT1*. Several series of 35 plants per genotype were observed throughout development. Wild-type, *psat1-1*, and *psat1-2* plants grew almost identically until they started to bolt (around 2 months after sowing; for plant growth conditions, see "Materials and Methods"). From that stage on, the rosette leaves of *psat1-1* and *psat1-2* senesced faster than equivalent wild-type leaves. About 2.5 months after germination, the oldest *psat1-1* and *psat1-2* mutant leaves started to turn yellow (Fig. 3A). Then they became pale brown and finally dried out as typical senescing leaves. Three months after germination, most of the rosette leaves from the mutants (except a few leaves from central verticils) underwent complete senescence, whereas most of the wild-type rosette leaves remained green (Fig. 3, B–D). It is noteworthy that the premature senescence phenotype was stronger in *psat1-2* than in *psat1-1*, as is the case for the biochemical phenotype: the reduction in the SE content was in fact more severe in *psat1-2* than in *psat1-1* (Fig. 2B). We then transformed *psat1-1* and *psat1-2* mutants with a T-DNA comprising a *Pro-35S*::*PSAT1* transgene. Homozygous complemented transgenic lines named D128 and D129 had a morphological phenotype indistinct from that of the wild type, thus demonstrating that an elevated level of PSAT1 restored normal leaf ontogeny (Fig. 3E). Interestingly, the level of *PSAT1* transgene overexpression was identical in wild-type, *psat1-1* (line D128; Fig. 3F), and *psat1-2* (line D129; data not shown) backgrounds. Whereas in the latter case this *PSAT1* expression level enabled complementation, it did not result in an elevated SE level in leaves compared with the wild type (Fig. 2B). Bolting, seed setting, seed yield,

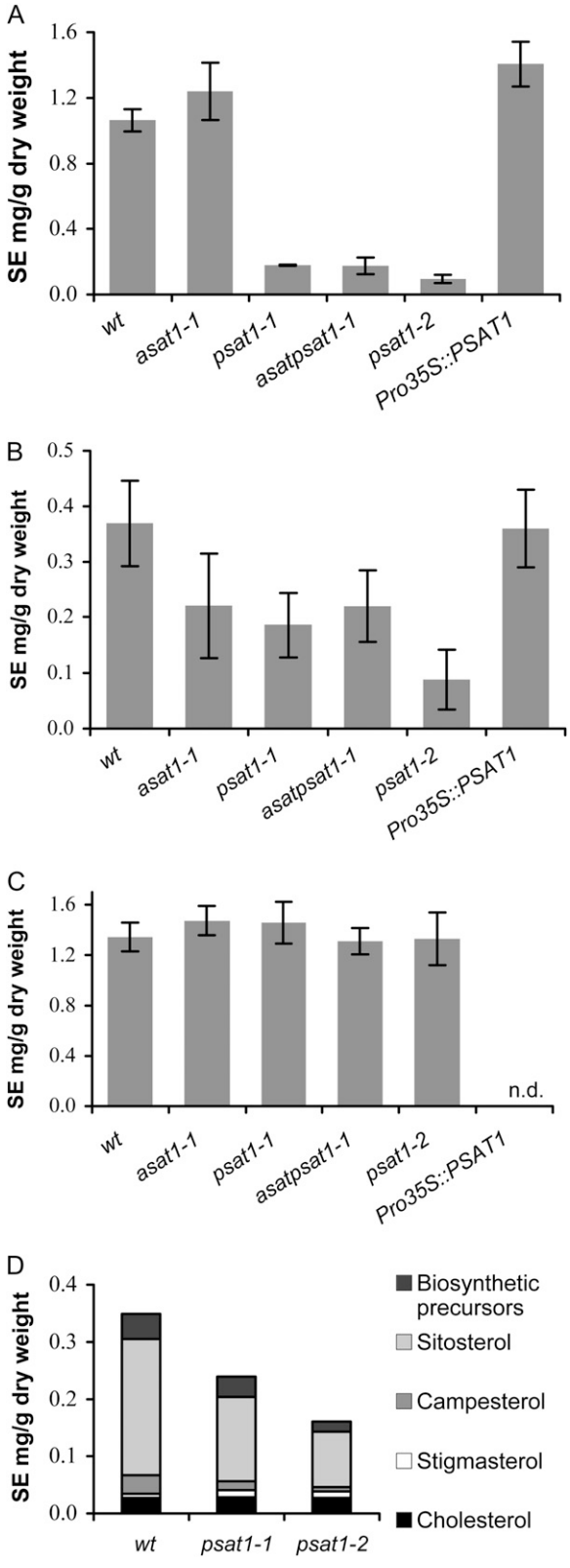

Figure 2. A to C, SE content of seeds (A), rosette leaves (B), and flowers (C) of wild-type (*wt*), *asat1-1*, *psat1-1*, *asatpsat1-1*, and *psat1-2* lines and of a *Pro-35S::PSAT1* Arabidopsis line in the wild-type background. Data for *asatpsat1-2* mutants, which are nearly identical to data for *psat1-2*, are not shown for simplification of the figure. D, Sterol composition of SE fractions from rosette leaves of wild-type, *psat1-1*, and *psat1-2* lines. For the sampling, lipid extraction, sterol analysis, and sterol content determination, see "Materials and Methods." n.d., Not determined. Biosynthetic precursors include cycloartenol, 24-methylene cycloartanol, Δ^7-avenasterol, Δ^7-sitosterol, 24-methylene cholesterol, and isofucosterol.

and seed germination rates were similar in the wild type and both *psat1-1* and *psat1-2* mutants (data not shown). It is also noteworthy that *asat1-1* mutant plants displayed no obvious phenotypic differences when compared with the wild type and that the double mutants *asatpsat1-1* and *asatpsat1-2* behaved exactly as the *psat1-1* and *psat1-2* lines did, respectively (Supplemental Fig. S4). In order to see whether the early leaf senescence phenotype of *psat1-1* and *psat1-2* plants was only due to a shift of the developmental time point after which senescence takes place in leaf ontogeny (i.e. natural senescence) or to some other effect on the genetic regulation of the leaf senescence process (Lim et al., 2003), we performed an induced senescence assay on detached leaves incubated in permanent darkness. In this assay, we observed an initiation and progression of senescence (i.e. chlorophyll degradation, progressive yellowing) that occurred at the same pace for wild-type and both *psat1-1* and *psat1-2* genotypes within 7 d of incubation (data not shown). This indicates that the underpinning molecular mechanisms acting on senescence had not been modulated by the *psat1-1* and *psat1-2* mutations.

We further analyzed the SE content of leaves and the expression levels of various genes with respect to developmental aging. Because chlorophyll degradation is a prominent process of leaf senescence (Hörtensteiner, 1999; Pružinská et al., 2005), developmental aging was monitored here by leaf yellowing. To reduce heterogeneity of leaf developmental stages in Arabidopsis rosettes due to the sequential senescence from older to younger leaves as documented (Hensel et al., 1993; Zentgraf et al., 2004; Panchuk et al., 2005), we detached equivalent leaves taken from wild-type, *psat1-1*, and *psat1-2* rosettes and incubated them in water in the same conditions as the plants from which they were taken (see "Materials and Methods"). Several assays performed with different batches of plants showed that wild-type leaves stayed greener than *psat1-1* or *psat1-2* leaves after the same time of incubation. The morphological phenotype of the detached wild-type leaves (Fig. 4A, left) and *psat1-2* leaves (Fig. 4A, right) after 20 d in water (the end of the experimental time frame for this assay) is shown. Indeed, about 20 d of incubation was necessary to measure 30% of nongreen wild-type leaf surface by leaf imaging (Fig. 4B); at this time point, *psat1-1* and *psat1-2* leaves showed more than 60% of nongreen leaf surface (note that the leaf yellowing curves of *psat1-1* and *psat1-2* were not completely superimposed, indicative again of a difference in the intensity of the phenotypes

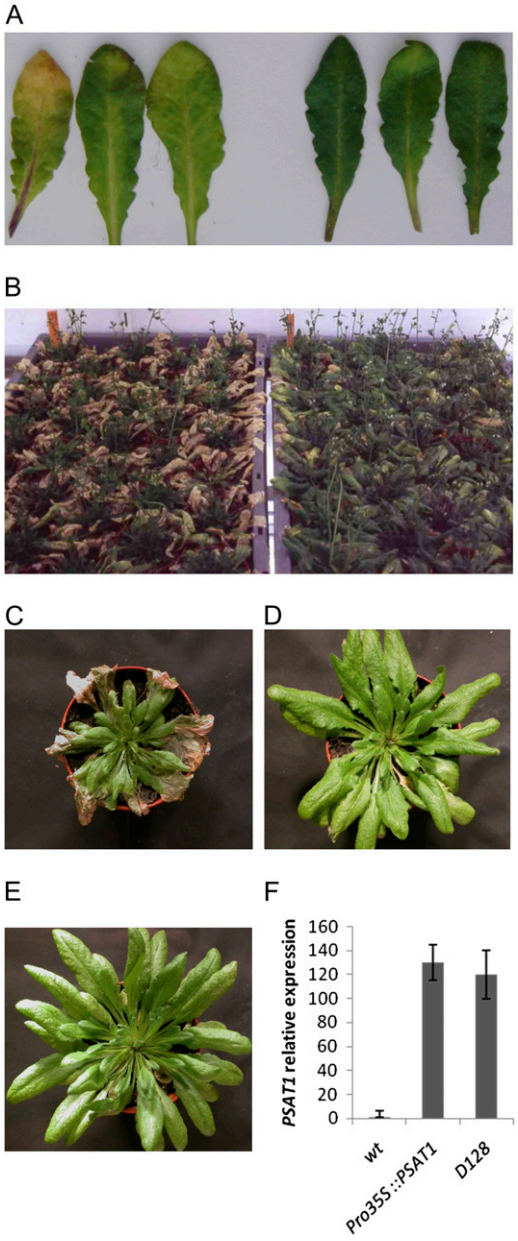

Figure 3. Early leaf senescence phenotype of *psat1* mutants from bolting stage on. A, Two and a half months after sowing, three representative rosette leaves from the external verticils of *psat1-1* plants (left) and wild-type plants (right). B, Three months after sowing, comparative view of *psat1-2* (left) and wild-type (right) plant trays. C to E, Three months after sowing, top view of plants from the *psat1-2*, wild-type, and *Pro-35S*::*PSAT1*-transformed *psat1-1* mutant (named D128) lines, respectively. Stems were cut off for clarity. Note that *asat1-1* mutant plants, which are not shown here, have the same morphological phenotype as the wild type (D). Note also that double mutants *asatpsat1-1* and *asatpsat1-2*, which are not shown here, have the same morphological phenotype as *psat1-1* and *psat1-2* mutant plants, respectively. F, Relative *PSAT1* expression measured by quantitative PCR in a *Pro-35S*::*PSAT1* line in the wild-type (*wt*) background and in the D128 *Pro-35S*::*PSAT1*-transformed *psat1-1* mutant, compared with the wild type.

associated with *psat1-1* and *psat1-2* mutations). In order to minimize possible deleterious effects of advanced senescence on analyses, we collected leaves at the time they were detached and 10 to 15 d later. Figure 4C shows the evolution of SE content of wild-type, *psat1-1*, and *psat1-2* leaves. These experiments indicated that SE increased with aging in wild-type leaves, whereas this metabolic process was severely hampered in *psat1-1* and *psat1-2* mutants. Interestingly, the lack of SE increase was more severe for *psat1-2* than for *psat1-1*. Finally, in order to see whether an elevated *PSAT1* expression level was associated with aging of wild-type leaves, we performed a quantitative PCR gene expression measurement for a set of targets including *PSAT1*, *ASAT1*, *Diacylglycerol Acyltransferase1* (*DGAT1*), *3-Hydroxy-3-Methylglutaryl-Coenzyme A Reductase* (*HMGR1*), and the senescence-associated genes *SAG101*, a gene encoding an acyl hydrolase involved in premature leaf senescence when overexpressed (He and Gan, 2002), and *SAG12*, a protease that is a known marker of natural senescence (Noh and Amasino, 1999). While *SAG12* was peaking from day 7 on (data not shown), indicating the beginning of the senescence process, the other genes had an almost unchanged expression except *PSAT1* and *SAG101*, which exhibited 2.5- and 3-fold increases at day 15, respectively (Fig. 4D; Supplemental Table S2). At this time, the wild-type leaf yellowing surface (i.e. nongreen surface measured by imaging) was about 10% to 15% of the total surface (Fig. 4B).

PSAT1 Is an Essential SE-Forming Enzyme in Arabidopsis Leaves and Seeds But Not in Flowers

To assess the capability of Arabidopsis leaves to cope with an increased biosynthetic flux in the so-called mevalonate pathway (ending up with SE ultimately), we fed wild-type, *asat1-1*, *psat1-1*, and *psat1-2* plants with exogenously supplied metabolic precursors. In the first experiment, we fed mevalonolactone, the lactonized form of mevalonic acid, to rosette leaves of growth chamber-grown plants. The strong and immediate toxicity of foliar applications of mevalonolactone to all lines prompted us to apply this precursor to young seedlings cultivated in synthetic liquid medium. A millimolar range of mevalonolactone concentrations was used to treat the seedlings. After 15 d of culture, wild-type plantlets were partly affected by 3 mM mevalonolactone (with a dry weight of about 45% of that of the control culture without mevalonolactone), whereas the same concentration was highly toxic to the *psat1-1* and *psat1-2* mutants (with a dry weight reduced to 4% of the control; Fig. 5A). Free and esterified sterol analysis indicated that wild-type SE levels increased along the range of mevalonolactone concentration in the medium, while the level of free sterols did not vary much. On the other hand, *psat1-1* and *psat1-2* SE levels remained close to control values along the same range of mevalonolactone concentrations, whereas their levels of free sterols were in-

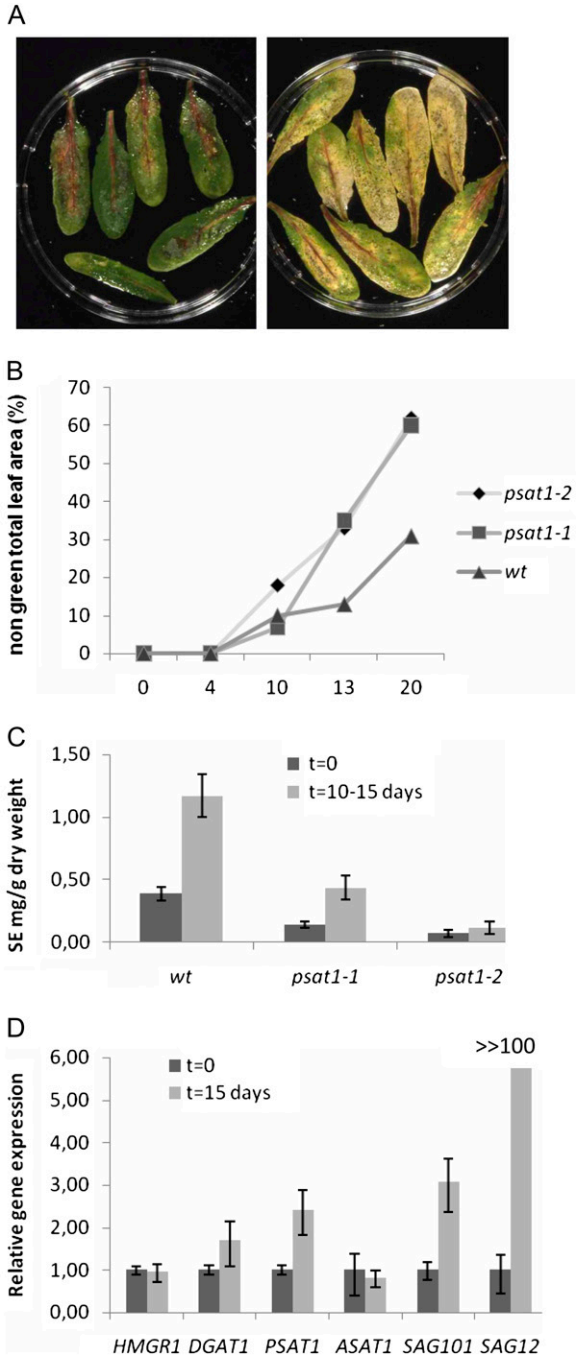

Figure 4. Progression of senescence in rosette leaves from wild-type (*wt*), *psat1-1*, and *psat1-2* lines. Fully expanded rosette leaves of about 4 to 6 cm in length were detached before bolting. A set of 20 to 30 leaves was stored at −80°C (time 0 [t=0] control), and 20 to 30 leaves were placed upon deionized water in several petri dishes in the growth chamber. A, Representative image of this "detached leaf assay" at the end of the time frame chosen for the experiment, showing the top view of wild-type (left) and *psat1-2* (right) leaves after 20 d in water. B, Progression of senescence determined by leaf imaging combined with computer-based quantification of greenness and nongreenness. The extent of senescence is expressed as a percentage of nongreen total leaf area (see "Materials and Methods"). A curve from one representative experiment is shown. C, Mutant *psat1-1* and *psat1-2* leaves were collected for SE measurement at the time they were detached (time 0) and when the nongreen surface reached 30% to 40% of the total leaf surface (10–15 d according to the experiment). Wild-type leaves were collected concomitantly. At that time (10–15 d), they were 10% to 15% nongreen in total surface. Data represent means and SD from three experiments where each sample was analyzed in duplicate. D, Expression in wild-type leaves of lipid biosynthetic genes considered in this study at the same stage (15 d) relative to time 0. Gene expression is calculated relative to *ACTIN2* (see "Materials and Methods").

creased (Fig. 5, B and C). Thus, exogenously added mevalonolactone was converted to SE in the wild type, in agreement with cellular free sterol homeostasis, whereas its uptake by the *psat1-1* and *psat1-2* mutants resulted in elevated free sterol levels, which probably disturbs this homeostasis and therefore causes the sensitivity to mevalonolactone.

Mevalonate, however, is a common precursor of many biosynthetic segments in the cytoplasmic isoprenoid pathway leading to key molecules such as cytokinins (Inoue et al., 2001). To gain specificity in these feeding experiments, we turned to squalene, which is the first committed precursor for sterol synthesis. Squalene (or squalane as a control) was spread on the rosette center and on young leaves from 2-month-old plants (fully expanded rosette stage). Three applications (10 μL each) were carried out at 5-d intervals. Such a treatment had no morphological or developmental effect on wild-type or *asat1-1* plants, whereas it severely affected the *psat1-1* and *psat1-2* mutants, which exhibited necrotic leaves 4 to 8 d after the treatment (Fig. 6A) and would finally die without bolting when left in the growth chamber. It is noteworthy that squalane, the hydrogenated counterpart of squalene, had no effect on any Arabidopsis lines. Rosette leaves were collected about 10 d after the third and last squalene application and were then analyzed for their free sterol and SE contents. Squalene treatment resulted in a strong increase of the SE levels in the case of the wild-type and the *asat1-1* mutant, whereas it was minute in the case of *psat1-1* and null in the case of *psat1-2* (Fig. 6B). These results indicate that squalene is metabolized into sterols, at least in wild-type and *asat1-1* plants, and that PSAT1 is the essential SE-forming enzyme in Arabidopsis leaves. Under these conditions, the free sterol content of the wild type and the *asat1-1* mutant decreased slightly, whereas it remained unchanged in the *psat1-1* and *psat1-2* mutants (Fig. 6C).

When the squalene treatment was postponed until after the onset of bolting and the applications were restricted to rosette leaves, either at the same or lower dosage, the *psat1-1* and *psat1-2* mutant plants, although their rosette leaves turned slowly necrotic, could develop their inflorescences and complete their life cycle. Three weeks after the treatment, we observed that the cauline leaves of the treated mutant plants turned yellow and started to dry (Fig. 7C) much

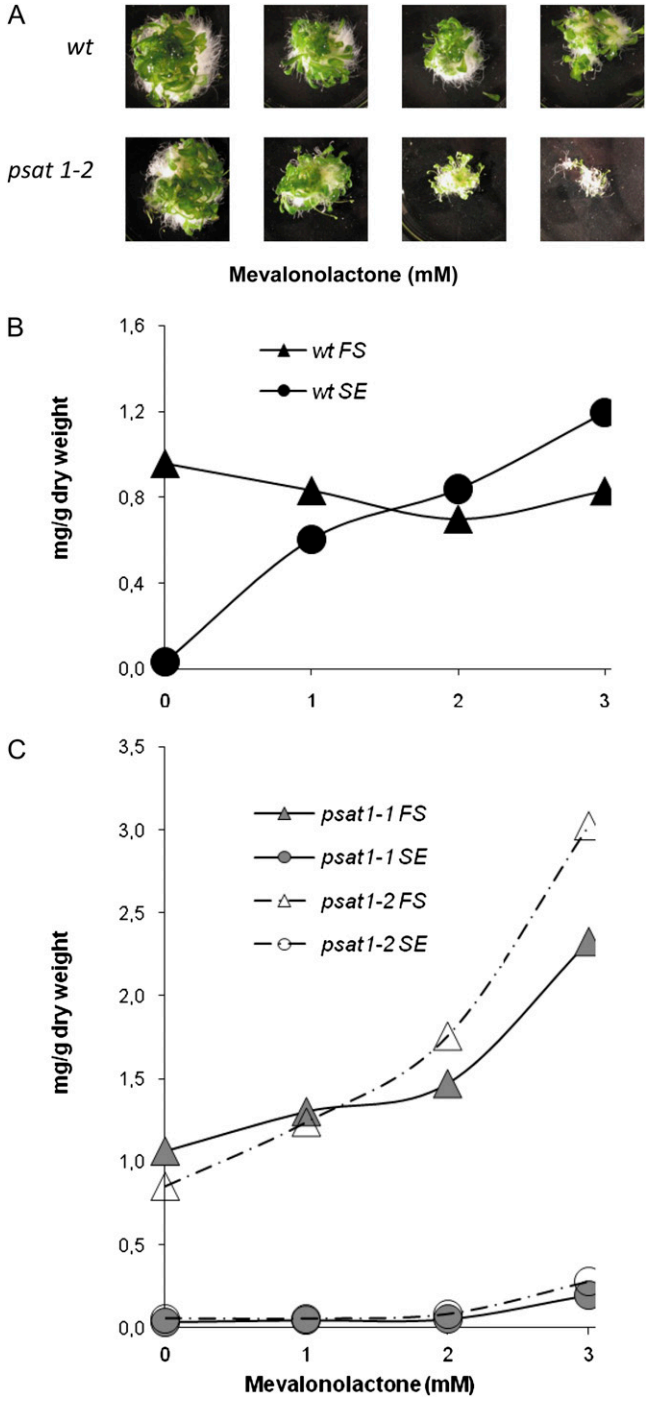

Figure 5. Effect of mevalonolactone on liquid medium-grown Arabidopsis plantlets. The *psat1-1* and *psat1-2* mutants and the wild type (*wt*) were germinated and grown for 2 weeks on solid Murashige and Skoog medium, then transferred to liquid medium in the absence or presence of mevalonolactone (1, 2, or 3 mM). Results shown are from a representative experiment from three similar ones. A, Top view of the wild-type and *psat1-2* plantlets 15 d after transfer. B and C (separated for clarity), SE and free sterol (*FS*) contents of the three lines versus mevalonolactone concentration.

earlier than the control mutant plants (Fig. 7B) or treated wild-type plants (Fig. 7A). Moreover, a delay in the silique development of the squalene-treated mutants was noticed, compared with the treated wild type or control mutants, suggesting a distal action of squalene in these lines. Furthermore, when lower limb epidermis peels from cauline leaves were stained with

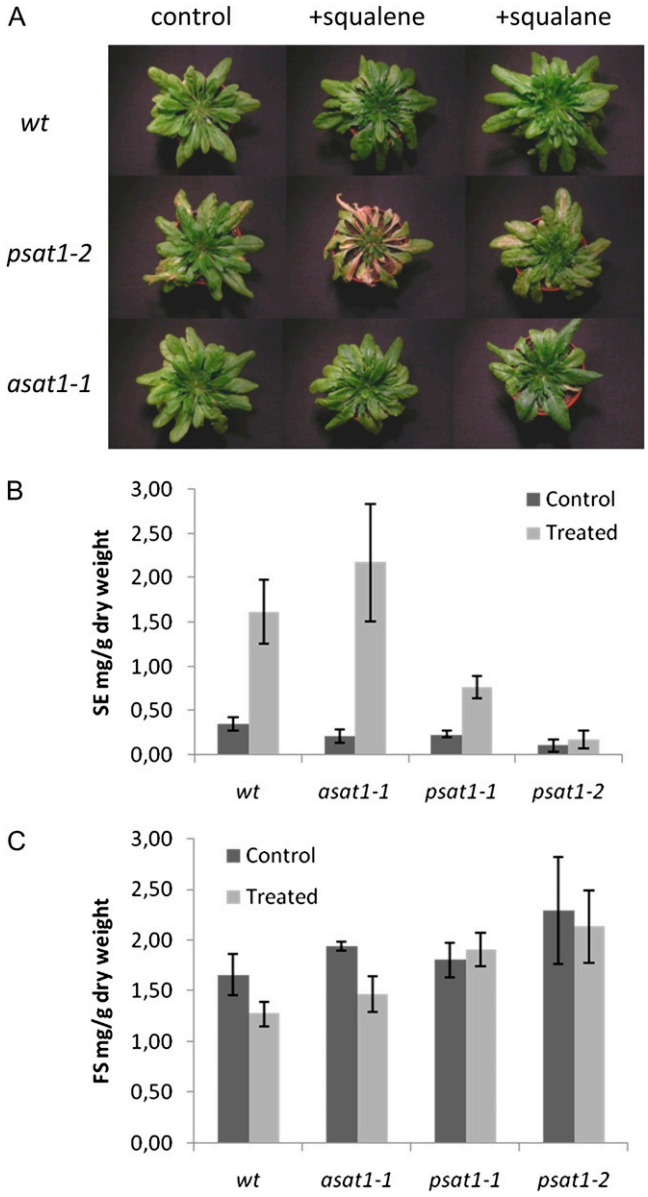

Figure 6. Effect of squalene on rosette leaves of Arabidopsis plants. Two-month-old plants from the wild-type (*wt*), *psat1-1*, *psat1-2*, and *asat1-1* lines were used. Squalene or squalane (10 μL) was applied three times at 5-d intervals on the rosette center and the five to seven youngest leaves. A, Top view of wild-type, *psat1-2*, and *asat1-1* plants 8 d after the third application (stems were cut off for clarity; note that the *psat1-1* plant phenotype is similar to that of *psat1-2*). B, SE content of control and squalene-treated plants. C, Free sterol (FS) content of control and squalene-treated plants.

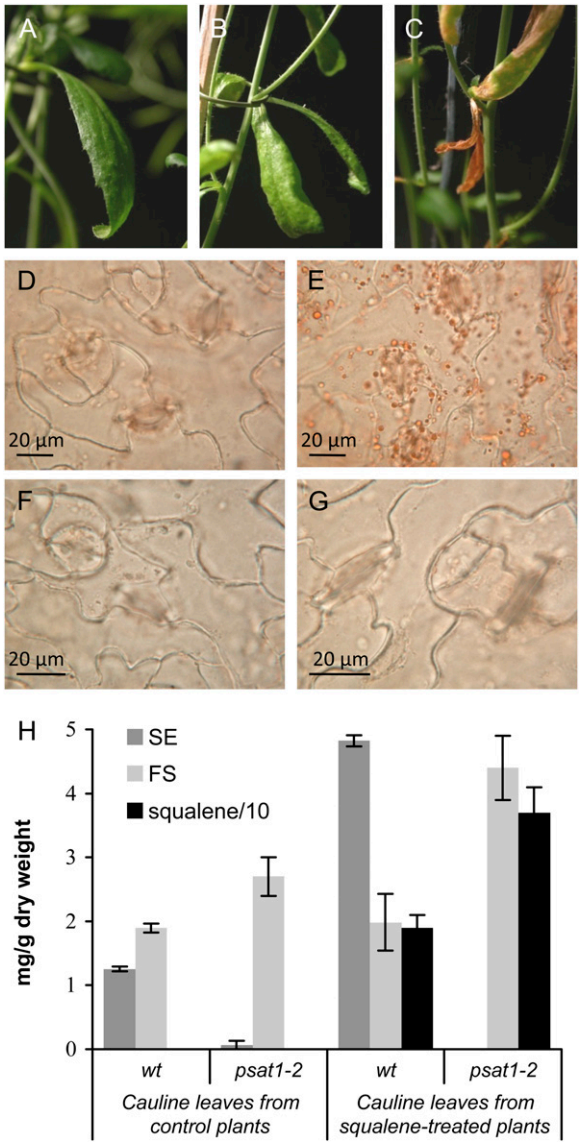

Figure 7. Effect of squalene on cauline leaves of Arabidopsis plants. In these experiments, special care was taken to restrict squalene applications to rosette leaves (excluding the rosette center). Two-and-a-half-month-old plants from wild-type, *psat1-1*, and *psat1-2* lines bearing short growing stems (around 4 cm high) received one application of squalene (5 μL). A to C, Photographs of cauline leaves at the third internode from the bottom of the stem, 25 d after the treatment, of treated wild-type (A), control *psat1-1* (B), and treated *psat1-1* (C) plants. D to G, At the same stage, lower epidermis peels from cauline leaves were stained with Sudan IV, then observed by light microscopy. Micrographs are from control wild-type plant (D), treated wild-type plant (E), control *psat1-1* plant (F), and treated *psat1-1* plant (G). Images in A to C, F, and G are representative of both *psat1-1* and *psat1-2* mutant plants. H, SE, free sterols (FS), and squalene contents of cauline leaves. Two-month-old and 1-week-old plants from wild-type (*wt*) and *psat1-2* lines showing 1- to 3-cm-high stems were treated three times at 5-d intervals by squalene (10 μL). Cauline leaves were collected 25 d after the first treatment, then freeze dried for analysis. Note that the black bars represent the squalene content divided by 10.

the neutral lipid dye Sudan IV and observed by light microscopy, the epidermis cells from the squalene-treated wild-type and *asat1-1* plants contained numerous red-orange globuli, while those from the *psat1-1* and *psat1-2* mutants were devoid of such structures (Fig. 7, D–G). It must be pointed out that the same lipid droplets were observed in lower limb epidermis cells from rosette leaves, either the squalene-spread or younger ones, in the case of wild-type and *asat1-1* lines but not in the *psat1-1* and *psat1-2* lines (data not shown). These intracellular oily droplets are probably made up of SE, since (1) the squalane treatment did not produce any intracellular droplets in any lines, (2) free sterols are not stained by Sudan IV, and (3) such droplets have been described in several plant systems overproducing sterols in the form of SEs (Gondet et al., 1994; Schaller et al., 1995). Finally, we performed squalene, SE, and free sterol measurements of these cauline leaves (Fig. 7H). Squalene, which is undetectable in control plants, accumulated in huge amounts in the cauline leaves of all squalene-treated plants: around 20 and 40 mg squalene g^{-1} dry weight for wild-type and *psat1-2* lines, respectively. Similar measurements on the corresponding stems indicated the same or higher squalene contents (data not shown). This demonstrates that squalene is mobilized and transported into the plant stem tissues. In agreement with this, our microscopic observations pointed out the presence of circulating large oily droplets in the apoplast of treated tissues (Supplemental Fig. S5). The SE level of wild-type cauline leaves was strongly increased by the treatment, in agreement with the observation of oily droplets in those leaves (Fig. 7, E and H). Conversely, the SE content of cauline leaves from *psat1-2* plants was shown to be very low, both in control and treated plants, whereas their free sterol content was almost doubled by the treatment (Fig. 7H). Taken together, these observations strongly suggest that it is the increased metabolic flux toward sterols, promoted by the squalene incorporation, that hampers silique formation in the case of the *psat1-1* and *psat1-2* mutants. Consequently, PSAT1 seems also to be the essential SE-forming enzyme in Arabidopsis seeds, in agreement with the very low SE content of seeds from the two *psat1* mutant lines (Fig. 2A).

Overexpression of PSAT1 from a *Pro35S::PSAT1* Transgene Is Not Sufficient to Trigger an Accumulation of SE in Plants

To assess whether the PSAT1 was able to trigger/pull the metabolic flux toward the accumulation of SE in plants, we transformed tobacco (*Nicotiana tabacum*) with a *Pro-35S::PSAT1* transgene. In this experiment, we used a wild-type tobacco genotype and a sterol-overproducing mutant (named *sterol overproduction* [*sterov*]) of the same genetic background previously isolated in a mutagenesis experiment (Schaller et al., 1993). In the case of both wild-type and *sterov* geno-

types, we measured a very strong accumulation of PSAT1 mRNA using quantitative PCR (data not shown). We then measured levels of total sterols and found no significant increase in transgenic plants compared with untransformed controls (Supplemental Fig. S3). This result shows that although being an essential component of sterol homeostasis, the *PSAT1* gene when overexpressed in tobacco cannot trigger an elevated biosynthetic flux in the sterol pathway and therefore is not a limiting enzyme in this pathway, at least in leaves. The same absence of SE increase was seen in leaves of the Arabidopsis *Pro-35S*::*PSAT1* line (Fig. 2B, last bar; Noiriel, 2004) or in seeds of *ProNAPIN*::*PSAT1* Arabidopsis (this work; data not shown).

DISCUSSION

Sterol acylation is an essential process of sterol homeostasis in eukaryotic cells. This has been extensively documented in yeast cells (Wagner and Daum, 2005; Daum et al., 2007) and mammalian cells (Temel et al., 2003). In plants, two enzymes of Arabidopsis have been characterized. PSAT1 catalyzes a phospholipid-dependent (acyl-CoA-independent) formation of SE (Banas et al., 2005). Recently, Chen et al. (2007) demonstrated the involvement of ASAT1, an acyl-CoA:sterol acyltransferase, in sterol esterification by expressing the corresponding gene both in yeast and in planta, where they showed that the SE content of Arabidopsis seeds expressing an *ASAT1* cDNA driven by a *NAPIN* promoter was about 2-fold higher than that of wild-type seeds. We performed here a detailed analysis of the SE content of *psat1-1*, *psat1-2*, and *asat1-1* deficient mutant lines. The comparison of the SE content of seeds from these lines with that of the wild-type seeds clearly showed that ASAT1 is not implicated in the physiological formation of SE during seed maturation, whereas PSAT1 appeared to be the main enzyme involved therein. The small amount of SE remaining in the *psat1-1* and *psat1-2* mutant seeds was probably due to the presence of residual PSAT1 protein in these mutants, as was suggested by the detection of low levels of gene expression in RT-PCR experiments. The fact that *asat1-1* mutants did not show any phenotype might be due to the expression of *ASAT1*-related genes present in the Arabidopsis genome (Hofmann, 2000). The depletion of SE in *psat1-1* and *psat1-2* mutant seeds does not affect seed germination and viability and moreover does not modify the accumulation of triacylglycerols, suggesting the occurrence of independent pathways for the accumulation of SE and triacylglycerols in Arabidopsis seeds. Conversely, Arabidopsis seeds from the *TAG1* mutant deficient in *DGAT1* had a reduced triacylglycerol content and no apparent effect on SE content but delayed seed development (Zou et al., 1999). We showed that in flowers, the SE content was equivalent in all the mutant lines, ruling out a significant role of ASAT1 or PSAT1 in SE production in developing flowers. This implies the existence of at least one flower-specific sterol acyltransferase, which remains to be identified. It is noteworthy that Arabidopsis flowers and pollen are particularly rich in SE, half of which are made of pollinastanol, 31-nor cycloartenol, 31-nor cycloartanol, and other 9β,19-cyclopropylsterols (Hernández-Pinzón et al., 1999; Wu et al., 1999; this work; data not shown). These flower-specific SE might be involved in pollination (Murphy, 2006). Compared with the SE levels of wild-type Arabidopsis seeds and flowers, that of wild-type leaves is quite low, which made the comparison with the SE content of mutant lines more difficult (see error bars in Fig. 2B). However, it appears that all the mutant lines have a lower SE content in leaves, the lowest for *psat1-2*. Thus, both ASAT1 and PSAT1 seemed to be involved in SE formation in leaves. Their respective roles in these organs were further revealed by treatments with metabolic precursors.

In plants, the sterol esterification process in conditions of increased metabolic flux toward sterols has been well documented (Maillot-Vernier et al., 1991; Gondet et al., 1994; Wilkinson et al., 1994; Schaller et al., 1995). Taking these previous studies into account, we used mevalonolactone to test the resistance of the *psat1-1* and *psat1-2* growing plantlets in liquid medium to an increased metabolic flux toward sterols. The data clearly demonstrate the greater sensitivity of the PSAT1-deficient lines to mevalonolactone compared with the wild type. Indeed, they could not transform the overproduced sterols into their ester form, whereas the wild-type plantlets could. In autotrophy, we tested the *asat1-1*, *psat1-1*, and *psat1-2* mutant lines for their resistance to squalene, the first committed precursor of sterols, which has been used to complement biochemical isoprenoid mutants (Suzuki et al., 2004; Okada et al., 2008). Such a squalene treatment was lethal for the two *psat1* lines but harmless for *asat1-1* as well as the wild-type lines, which could transform the excess of synthesized sterols into their SE derivatives stored in lipid droplets, whereas the *psat1-1* mutant could hardly and the *psat1-2* mutant could not at all. These data clearly show the predominance of PSAT1 over ASAT1 in controlling the free sterol content of rosette leaves. Shifting the squalene treatment of rosette leaves after the onset of bolting allowed the further development of *psat1-1* and *psat1-2* plants and the observation of SE accumulation in wild-type cauline leaves, suggesting a mobilization and transport of squalene. The discrepancy between free sterol levels in rosette leaves (Fig. 6C) and cauline leaves (Fig. 7H) of squalene-treated *psat1-2* mutants might be due to the difference in duration of squalene treatment before analysis (8–10 d and 25 d, respectively). Furthermore, we suggest that a strong increase of free sterols upon squalene feeding of *psat1-2* mutant leaves could be the direct consequence of the PSAT1 loss of function. Indeed, previous studies showed in vitro that end product (24-alkyl-Δ^5-sterols)-activated PSAT1 esterified sterol intermediates efficiently (Banas et al., 2005). This

could result in vivo in the maintenance of membrane free sterols in physiological concentrations and ultimately would give to PSAT1 the role of a cellular sensor of free sterols, which remained to be further documented.

Besides the essential role of PSAT1 in leaf sterol homeostasis, our results also point to its possible role in leaf senescence. We consistently observed an early senescence phenotype of the *psat1-1* and *psat1-2* mutant lines, which could be complemented by *PSAT1* overexpression. This senescence phenotype was studied with detached leaves incubated in water. The SE content of the wild-type leaves after 10 to 15 d in water was shown to be triple that of freshly detached leaves, reaching more than 1 mg per gram dry weight, whereas those of *psat1-1* and *psat1-2* remained much lower. Gene expression measurements performed on wild-type detached leaves showed that the expression of *PSAT1* was increased, during this aging experiment, by a factor of about 2 to 3, similar to that of *SAG 101*, an acyl hydrolase gene known as a senescence-associated gene (He and Gan, 2002), whereas *HMGR1* and *ASAT1* expression levels remained unchanged. The fact that the expression of *HMGR1*, a regulatory gene acting on sterol accumulation, remained unchanged could indicate that the increase of SE was not due to an increased biosynthetic flux in the mevalonate pathway but rather to sterol interconversion, within the time frame of the experiment. Our observations are reminiscent of older studies describing an increase in SE content during aging of cotyledons, leaves, or roots of various species (Dyas and Goad, 1993, and refs. therein). McKegney et al. (1995) studied senescing bean (*Phaseolus vulgaris*) cotyledons and isolated cytosolic particles that they showed to be strongly enriched in SE, wax esters, and (to a lesser extent) free fatty acids relative to microsomal membranes. The authors concluded that blebbing of cytosolic particles from membranes is a means of removing phospholipid catabolites during senescence. It is known also that developmental aging of leaves results in their conversion of nutrient sinks to nutrient sources, and this is accompanied by changes in cellular lipid metabolism. Kaup et al. (2002) compared young and senescent leaves directly taken from soil-growing plants and described an increase of triacylglycerol content with advancing leaf senescence, accompanied by an increase in *DGAT1* transcript and protein levels. They found that in senescing leaves, DGAT1 was associated with chloroplast membranes and that triacylglycerols accumulating in these leaves were enriched in galactolipid-specific fatty acids. These authors concluded that DGAT1 plays a role in senescence by sequestering fatty acids released during catabolism of galactolipids and proposed that it could be an intermediate step in the conversion of thylakoid fatty acids to phloem-mobile Suc during leaf senescence (Kaup et al., 2002). A similar process might well occur in the cytoplasmic compartment of leaf cells. Indeed, the formerly described sterol acyltransferase activities (Dyas and Goad, 1993; Bouvier-Navé and Benveniste, 1995) and the recently characterized PSAT1 (Banas et al., 2005) were consistently found associated with the microsomal membranes. Therefore, the premature leaf senescence phenotype exhibited by the *psat1-1* and *psat1-2* lines and the concomitant increase of SE content of wild-type leaves strongly suggest that PSAT1 would take part in the recycling of both the phospholipid fatty acids and the free sterols released from inner cellular membranes as senescence progresses. Finally, the early leaf senescence phenotype of *psat1* mutants is reminiscent of that of mutants impaired in vacuolar autophagy, a major process of nutrient recycling (Xiong et al., 2005). Further research efforts will be devoted to the physiological implication of PSAT1, particularly when plants are facing environmental stresses (Hugly et al., 1990; Murata et al., 1992).

MATERIALS AND METHODS

Plant Growth and Transformation Conditions

Arabidopsis (*Arabidopsis thaliana*) T-DNA insertional mutant and other transgenic lines described here are in the Columbia-0 background. Plants were grown in a controlled growth chamber in standard horticultural soil with a 12-h-light/12-h-dark regime at 21°C during the light period and 19°C during the dark period. Relative humidity was 60% to 80%, and photon fluence rate from white fluorescent tubes was 60 μmol m^{-2} s^{-1} at the level of rosettes (Babiychuk et al., 2008). For germination of Arabidopsis on synthetic medium to analyze segregation of a given marker gene carried on a T-DNA, seeds were wetted with 70% ethanol, surface sterilized with a 25% commercial solution of sodium hypochlorite, rinsed three times with sterile water, and sown on Murashige and Skoog salts medium containing 1% Suc. Plates were stored for 48 h at 4°C in the dark for stratification and then transferred in a controlled growth chamber with a 16-h-light/8-h-dark regime at 23°C during the light period and 21°C during the dark period. *Agrobacterium tumefaciens*-mediated transformation of wild-type Arabidopsis plants by a floral dip method was described (Clough and Bent, 1998). Specific genetic crossings were carried out to generate lines carrying *psat1-1* or *psat1-2* and *asat1* alleles at a homozygous ploidy level.

Tobacco (*Nicotiana tabacum*) wild-type, *sterov*, and *Pro-35S::PSAT1* plants were grown in a controlled growth chamber in standard horticultural soil with a 16-h-light/8-h-dark regime at 24°C during the light period and 20°C during the dark period. Relative humidity was 70% to 90%, and photon fluence rate from white fluorescent tubes was 60 μmol m^{-2} s^{-1} at the level of bottom leaves. F1 hybrids were generated by specific genetic crossing of wild-type, *sterov*, and *Pro-35S::PSAT1* line K1018 plants (which carried a T-DNA insertion at a single locus), as shown by Mendelian segregation analysis.

Insertional Mutant Isolation and Characterization

The Arabidopsis T-DNA insertion mutant lines SALK_037289 and SALK_117091, renamed *psat1-1* and *psat1-2* mutants, were identified at http://signal.salk.edu/cgi-bin/tdnaexpress (Alonso et al., 2003; Banas et al., 2005). A T-DNA insertion in At5g23190 was identified in the GABI-Kat collection at www.gabi-kat.de. The line was named *asat1-1*. Individual seeds from all lines analyzed herein were grown in vitro as described above in order to assess their genotype according to standard genomic PCR procedures. Oligonucleotides used to prime the PCR in this genotype screen are given in Supplemental Table S1. The quantification of *PSAT1* and *ASAT1* transcripts was performed in homozygous wild-type or mutant plants by RT-PCR.

Semiquantitative and Quantitative Real-Time RT-PCR Analysis

Total leaf RNA samples from plants grown in horticultural conditions or in detached leaf-aging assays were isolated with TRIzol reagent (Life Technol-

ogies) according to the technical specifications given by the manufacturer. The semiquantitative RT-PCR analyses used to verify the expression of *PSAT1*, *ASAT1*, and *ACTIN2* (an accepted housekeeping gene) in the knockout mutant lines were performed using the SuperScript III One-Step RT-PCR system with Platinum *Taq* DNA polymerase (Invitrogen) or with a standard *Taq* DNA polymerase with 200 ng of RNA (DNase I treated) in each reaction according to the specifications given by the manufacturer. Primer sequences for *PSAT1*, *ASAT1*, and *ACTIN2* (At5g09810) amplifications are given in Supplemental Table S1. The thermocycling was 5 min at 95°C, then 35 cycles of 30 s of denaturation at 95°C, 45 s of primer hybridization at 55°C, and 2 min of elongation at 72°C. The RT reaction prior to real-time quantitative PCR analysis of gene expression was done with the SuperScript III First Strand cDNA Synthesis Kit (Invitrogen) using 1 μg of total RNA and 100 ng of random hexamers (Boehringer) following instructions provided by the manufacturer. Real-time PCR measurements were done with a GeneAmp 5700 Sequence Detection System (Applied Biosystems). Primers were designed with Primer Express software (Applied Biosystems), and their specificity was verified with a BLAST analysis and by the amplicon dissociation protocol of the GeneAmp5700 Sequence Detection System. Primer sequences for genes considered in this study are listed in Supplemental Table S1. PCR was done in a final volume of 25 μL with 300 nM final concentration of each primer and a commercial SYBR Green PCR mix concentrated 2-fold (Applied Biosystems). The PCR program included a 1-min denaturation step at 95°C, then 40 cycles of 15 s of denaturation at 95°C and 1 min of hybridization/polymerization at 60°C. Approximations of gene expression levels were calculated using the comparative threshold amplification cycle (Ct) method ($2^{-\Delta\Delta Ct}$) as described (Livak and Schmittgen, 2001). Gene expression measurements performed in wild-type detached leaves (Fig. 4D) were done under conditions that minimize RNA degradation, as shown by the stability of the Ct value for the housekeeping gene (*ACTIN2*) within the time frame of the assay (Supplemental Table S2).

Construction of a *Pro35S*::*PSAT1* Expression Vector

A 2-kb cDNA sequence of pGVp35S:*AtPSAT* (Banas et al., 2005) encoding the open reading frame of PSAT1 was subcloned directionally into the *Xba*I and *Xho*I restriction sites of a binary vector pBASTA carrying a phosphinothrycin resistance marker gene. The vector was transferred into *A. tumefaciens* LBA4404 by triparental mating, and transconjugants were checked by PCR.

Mevalonolactone and Squalene Treatment

Arabidopsis wild-type, *asat1-1*, *psat1-1*, and *psat1-2* lines were germinated on solid one-third-concentrated Murashige and Skoog salts and 1% Suc (w/w) at 24°C under 16-h-light/8-h-dark conditions. After 2 weeks, the plantlets were transferred into beakers containing liquid one-half-strength Murashige and Skoog salts and 1% Suc (10 plantlets into 100 mL). Mevalonolactone (Sigma) was then added to the medium as a 5 M ethanolic solution, so as to obtain 0, 1, 2, or 3 mM final concentration. The amount of ethanol added at the highest concentration (60 μL) was shown to have no effect on growth. The plantlets were grown for 2 more weeks under the same temperature and light conditions with shaking (120 rpm), then harvested and frozen. The squalene treatments were carried out on 2-month-old plants. The oldest leaves and the primary stem, if present, were cut off before the first squalene application. Ten microliters of squalene (or of squalane as a control; both from Sigma) was spread three times at 5-d intervals onto the five to seven youngest rosette leaves. Rosettes were collected about 10 d after the third application and frozen. Alternatively, the squalene treatment was postponed until after the onset of bolting (about 2.5-month-old plants) and restricted to young rosette leaves to enable the further development of *psat1-1* and *psat1-2* plants.

Light Microscopic Observations

Lipid staining of leaf epidermis was done with Sudan IV. Samples were collected freshly, suspended in a 70% ethanol solution containing 0.3% (w/v) of the dye, and observed with a Leitz microscope with bright-field illumination.

Aging of Detached Leaves

Fully expended rosette leaves (4–6 cm long) were detached. Sets of 20 to 30 leaves of wild-type, *psat1-1*, and *psat1-2* lines were stored at −80°C (time 0 controls), and others were placed upon deionized water in petri dishes in the growth chamber, either in the dark to compare induced senescence of the different lines or under normal light conditions to observe aging of the detached leaves. The yellowing rate (aging indicated by chlorophyll breakdown) of senescing leaves was measured as pixels by image processing. Petri dishes containing water-incubated leaves were imaged with a Nikon digital camera. Green versus nongreen leaf surface was measured using ImageJ version 1.43c (http://rsb.info.nih.gov/ij/) and the Threshold Color plugin version 1.9 (http://www.dentistery.bham.ac.uk/landing/).

Sterol and Triacylglycerol Analysis

Liquid nitrogen-frozen seeds were ground in a Microdismembrator (Sartorius) in the presence of glass beads at 3,000 rpm during 3 min, then freeze dried before extraction of lipids. Leaves and flowers were first freeze dried, suspended in the lipid extraction mixture, and ground using an Ultra-Turrax blender (Janke und Künkel, IKA Labortechnik). Extraction of lipids was carried out either in dichloromethane:methanol (2:1, v/v) under reflux, as described (Bouvier-Navé et al., 2000), or in chloroform:methanol (2:1, v/v) at 50°C. The extraction process (25–100 mg of dry material in 25–50 mL for 1 h) was repeated twice. Then the combined and concentrated extracts were submitted to thin-layer chromatography, the SE fractions were saponified, and the resulting sterols and the free sterol fractions were acetylated, purified, and submitted to gas chromatography-flame ionization detection analysis as described previously (Bouvier-Navé et al., 2000). Identification of compounds was confirmed by gas chromatography-mass spectrometry (Babiychuk et al., 2008). For the sterol content determination, each sample was analyzed in triplicate and the analysis was reproduced at least once on new biological samples from identical experiments. Mean values include both types of replicates, and error bars represent overall SD. Triacylglycerols were analyzed as described (Bouvier-Navé et al., 2000).

Supplemental Data

The following materials are available in the online version of this article.

Supplemental Figure S1. Isolation of loss-of-function mutants for *PSAT1* and *ASAT1*.

Supplemental Figure S2. Triacylglycerol contents of dry seeds from different lines considered in this study.

Supplemental Figure S3. Total sterols of tobacco cv Xanthi genotype SH6.

Supplemental Figure S4. Leaf phenotype of all lines studied in this work.

Supplemental Figure S5. Lower epidermis peels from growing leaves adjacent to rosette leaves that were spread with squalene.

Supplemental Table S1. PCR primers used in this study.

Supplemental Table S2. Real-time PCR quantification of *PSAT1* gene expression normalized to the expression of the housekeeping gene *ACTIN2* using the Ct method (Livak and Schmittgen, 2001).

ACKNOWLEDGMENTS

We thank Márta Ramel for outstanding horticultural work. We are indebted to Jitao Zou and Qilin Chen for providing the Arabidopsis *asat1-1* line originally obtained from GABI-Kat resources. We warmly thank Jérôme Mutterer for image processing. The *psat1-1* and *psat1-2* insertional lines were obtained from the Nottingham Arabidopsis Stock Centre.

Received August 17, 2009; accepted November 13, 2009; published November 18, 2009.

LITERATURE CITED

Alonso JM, Stepanova AN, Leisse TJ, Kim CJ, Chen H, Shinn P, Stevenson DK, Zimmerman J, Barajas P, Cheuk R, et al (2003) Genome-wide insertional mutagenesis of *Arabidopsis thaliana*. Science **301:** 653–657

Babiychuk E, Bouvier-Navé P, Compagnon V, Suzuki M, Muranaka T, Van Montagu M, Kushnir S, Schaller H (2008) Allelic mutant series reveal distinct functions for Arabidopsis cycloartenol synthase 1 in cell viability and plastid biogenesis. Proc Natl Acad Sci USA **105:** 3163–3168

Banas A, Carlsson AS, Huang B, Lenman M, Banas W, Lee M, Noiriel A, Benveniste P, Schaller H, Bouvier-Navé P, et al (2005) Cellular sterol ester synthesis in plants is performed by an enzyme (phospholipid: sterol acyltransferase) different from the yeast and mammalian acyl-CoA:sterol acyltransferase. J Biol Chem **280:** 34626–34634

Benveniste P (2004) Biosynthesis and accumulation of sterols. Annu Rev Plant Biol **55:** 429–457

Bloch KE (1983) Sterol structure and membrane function. CRC Crit Rev Biochem **14:** 47–92

Bouvier-Navé P, Benveniste P (1995) Sterol acyltransferase and steryl ester hydrolase activities in a tobacco mutant which overproduces sterols. Plant Sci **110:** 11–19

Bouvier-Navé P, Benveniste P, Oelkers P, Sturley SL, Schaller H (2000) Expression in yeast and tobacco of plant cDNAs encoding acyl CoA: diacylglycerol acyltransferase. Eur J Biochem **267:** 85–96

Chang TY, Chang CC, Cheng D (1997) Acyl-coenzyme A:cholesterol acyltransferase. Annu Rev Biochem **66:** 613–638

Chen Q, Steinhauer L, Hammerlindl J, Keller W, Zou J (2007) Biosynthesis of phytosterol esters: identification of a sterol O-acyltransferase in Arabidopsis. Plant Physiol **145:** 974–984

Clough SJ, Bent AF (1998) Floral dip: a simplified method for Agrobacterium-mediated transformation of Arabidopsis thaliana. Plant J **16:** 735–743

Daum G, Wagner A, Czabany T, Athenstaedt K (2007) Dynamics of neutral lipid storage and mobilization in yeast. Biochimie **89:** 243–248

Demel RA, De Kruyff B (1976) The function of sterols in membranes. Biochim Biophys Acta **457:** 109–132

Dyas L, Goad LJ (1993) Steryl fatty acyl esters in plants. Phytochemistry **34:** 17–29

Garcia RE, Mudd JB (1978a) Identification of an acyl donor in steryl ester biosynthesis by enzyme preparations from spinach leaves. Plant Physiol **62:** 348–353

Garcia RE, Mudd JB (1978b) Fatty acid and sterol specificity in the biosynthesis of steryl esters by enzyme preparations from spinach leaves. Arch Biochem Biophys **190:** 315–321

Gondet L, Bronner R, Benveniste P (1994) Regulation of sterol content in membranes by subcellular compartmentation of steryl-esters accumulating in a sterol-overproducing tobacco mutant. Plant Physiol **105:** 509–518

Hamilton JA, Small DM (1982) Solubilization and localization of cholesteryl oleate in egg phosphatidylcholine vesicles: a carbon 13 NMR study. J Biol Chem **257:** 7318–7321

He Y, Gan S (2002) A gene encoding an acyl hydrolase is involved in leaf senescence in *Arabidopsis*. Plant Cell **14:** 805–815

Hensel LL, Grbic V, Baumgarten DA, Bleeker AD (1993) Developmental and age-related processes that influence the longevity and senescence of photosynthetic tissues in *Arabidopsis*. Plant Cell **5:** 553–564

Hernández-Pinzón I, Ross JH, Barnes KA, Damant AP, Murphy DJ (1999) Composition and role of tapetal lipid bodies in the biogenesis of the pollen coat of Brassica napus. Planta **208:** 588–598

Hofmann K (2000) A superfamily of membrane-bound O-acyltransferases with implications for Wnt signaling. Trends Biochem Sci **25:** 111–112

Hörtensteiner S (1999) Chlorophyll breakdown in higher plants and algae. Cell Mol Life Sci **56:** 330–347

Hugly S, McCourt P, Browse J, Patterson GW, Somerville C (1990) A chilling sensitive mutant of Arabidopsis with altered steryl-ester metabolism. Plant Physiol **93:** 1053–1062

Inoue T, Higuchi M, Hashimoto Y, Seki M, Kobayashi M, Kato T, Tabata S, Shinozaki K, Kakimoto T (2001) Identification of CRE1 as a cytokinin receptor from Arabidopsis. Nature **409:** 1060–1063

Jonas A (2000) Lecithin cholesterol acyltransferase. Biochim Biophys Acta **1529:** 245–256

Kaup MT, Froese CD, Thompson JE (2002) A role for diacylglycerol acyltransferase during leaf senescence. Plant Physiol **129:** 1616–1626

Lewis TA, Rodriguez RJ, Parks LW (1987) Relationship between intracellular sterol content and sterol esterification and hydrolysis in Saccharomyces cerevisiae. Biochim Biophys Acta **921:** 205–212

Lim PO, Woo HR, Nam HG (2003) Molecular genetics of leaf senescence in Arabidopsis. Trends Plant Sci **8:** 272–278

Livak KL, Schmittgen TD (2001) Analysis of relative gene expression data using real-time quantitative PCR and the 2^{-}DDCt method. Methods **25:** 402–408

Maillot-Vernier P, Gondet L, Schaller H, Benveniste P, Belliard G (1991) Genetic study and further biochemical characterization of a tobacco mutant that overproduces sterols. Mol Gen Genet **231:** 33–40

McKegney G, Yao K, Ghosh S, Huff A, Mayak S, Thompson JE (1995) The lipid composition of cytosolic particles isolated from senescing bean cotyledons. Phytochemistry **39:** 1335–1345

Murata N, Ishizaki-Nishizawa O, Higashi S, Hayashi H, Tasaka Y, Nishida I (1992) Genetically engineered alteration in the chilling sensitivity of plants. Nature **356:** 710–713

Murphy DJ (2006) The extracellular pollen coat in members of the Brassicaceae: composition, biosynthesis, and functions in pollination. Protoplasma **228:** 31–39

Noh YS, Amasino RM (1999) Identification of a promoter region responsible for the senescence-specific expression of SAG12. Plant Mol Biol **41:** 181–194

Noiriel A (2004) Etude d'une famille de gènes d'Arabidopsis thaliana homologues de la lécithine cholestérol acyltransférase humaine: caractérisation d'une nouvelle phospholipase A1 et étude d'une stérol acyltransférase. PhD thesis. Université Louis Pasteur, Strasbourg, France

Okada K, Kasahara H, Yamaguchi S, Kawaide H, Kamiya Y, Nojiri H, Yamane H (2008) Genetic evidence for the role of isopentenyl diphosphate isomerases in the mevalonate pathway and plant development in Arabidopsis. Plant Cell Physiol **49:** 604–616

Panchuk II, Zentgraf U, Volkov RA (2005) Expression of the Apx gene family during leaf senescence of Arabidopsis thaliana. Planta **222:** 926–932

Pružinská A, Tanner G, Aubry S, Anders I, Moser S, Müller T, Ongania KH, Kraütler B, Youn JY, Liljegren SJ, et al (2005) Chlorophyll breakdown in senescent Arabidopsis leaves: characterization of chlorophyll catabolic enzymes involved in the degreening reaction. Plant Physiol **139:** 52–63

Roche Y, Gerbeau-Pissot P, Buhot B, Thomas D, Bonneau L, Gresti J, Mongrand S, Perrier-Cornet JM, Simon-Plas F (2008) Depletion of phytosterols from the plasma membrane provides evidence for disruption of lipid rafts. FASEB J **22:** 3980–3991

Schaller H (2004) New aspects of sterol biosynthesis in growth and development of higher plants. Plant Physiol Biochem **42:** 465–476

Schaller H, Grausem B, Benveniste P, Chye ML, Tan CT, Song YH, Chua NH (1995) Expression of the *Hevea brasiliensis* (H.B.K.) Mull. Arg. 3-hydroxy-3-methylglutaryl-coenzyme A reductase 1 in tobacco results in sterol overproduction. Plant Physiol **109:** 761–770

Schaller H, Maillot-Vernier P, Belliard G, Benveniste P (1993) Biochemical characterization of tobacco mutants resistant to azole fungicides and herbicides. Biochem Soc Trans **21:** 1052–1057

Schuler I, Milon A, Nakatani Y, Ourisson G, Albrecht A, Benveniste P, Hartman MA (1991) Differential effects of plant sterols on water permeability and on acyl chain ordering of soybean phosphatidylcholine bilayers. Proc Natl Acad Sci USA **88:** 6926–6930

Sturley SL (1997) Molecular aspects of intracellular sterol esterification: the acyl coenzyme A:cholesterol acyltransferase reaction. Curr Opin Lipidol **8:** 167–173

Suzuki M, Kamide Y, Nagata N, Seki H, Ohyama K, Kato H, Masuda K, Sato S, Kato T, Tabata S, et al (2004) Loss of function of 3-hydroxy-3-methylglutaryl coenzyme A reductase 1 (HMG1) in *Arabidopsis* leads to dwarfing, early senescence and male sterility, and reduced sterol levels. Plant J **37:** 750–761

Temel RE, Gebre AK, Parks JS, Rudel LL (2003) Compared with acyl-coA: cholesterol O-acyltransferase 1 and lecithin:cholesterol acyltransferase, ACAT2 displays the greatest capacity to differentiate cholesterol from sitosterol. J Biol Chem **278:** 47594–47601

Wagner A, Daum G (2005) Formation and mobilization of neutral lipids in the yeast *Saccharomyces cerevisiae*. Biochem Soc Trans **33:** 1174–1177

Wilkinson SC, Powls R, Goad J (1994) The effects of excess exogenous mevalonic acid on sterol and ester biosynthesis in celery (*Apium graveolens*) cell suspension culture. Phytochemistry **37:** 1031–1035

Wu SSH, Moreau RA, Whitaker BD, Huang HC (1999) Steryl esters in the elaioplasts of the tapetum in developing *Brassica* anthers and their recovery on the pollen surface. Lipids **34:** 517–523

Xiong Y, Contento AL, Bassham DC (2005) AtATG18a is required for the formation of autophagosomes during nutrient stress and senescence in Arabidopsis thaliana. Plant J **42:** 535–546

Yang H, Bard M, Bruner DA, Gleeson A, Deckelbaum RJ, Aljinovic G, Pohl TM, Rothstein R, Sturley SL (1996) Sterol esterification in yeast: a two-gene process. Science **272:** 1353–1356

Zentgraf U, Jobst J, Kolb D, Rentsch D (2004) Senescence related gene expression profiles of rosette leaves of *Arabidopsis thaliana*: leaf age versus plant age. Plant Biol **6:** 178–183

Zimowski J, Wojciechowski ZA (1981a) Acyl donors for sterol esterification by cell free preparations from Sinapis alba roots. Phytochemistry **20:** 1795–1798

Zimowski J, Wojciechowski ZA (1981b) Partial purification and specificity of triacylglycerol:sterol acyltransferase from *Sinapis alba*. Phytochemistry **20:** 1799–1803

Zou J, Wei Y, Jako C, Kumar A, Selvaraj G, Taylor D (1999) The *Arabidopsis thaliana* TAG1 mutant has a mutation in a diacylglycerol acyltransferase gene. Plant J **19:** 645–653